

# Germanium Photovoltaic Cells with MoO<sub>x</sub> Hole-Selective Contacts

A. Alcañiz<sup>(a)</sup>, G. López<sup>(a)</sup>, I. Martín<sup>(a)</sup>, A. Jiménez<sup>(b)</sup>, A. Datas<sup>(a,b)</sup>, E. Calle<sup>(a)</sup>, E. Ros<sup>(a)</sup>, L.G. Gerling<sup>(a)</sup>, C. Voz<sup>(a)</sup>, C. del Cañizo<sup>(b)</sup>, R. Alcubilla<sup>(a)</sup>

<sup>(a)</sup> Electronic Engineering Department, Universitat Politècnica de Catalunya, Jordi Girona 1-3, Barcelona 08034, Spain

<sup>(b)</sup> Instituto de Energía Solar, Universidad Politécnica de Madrid, 28040 Madrid, Spain.

**Keywords:** germanium, MoO<sub>x</sub>, transition metal oxide, solar cell, thermophotovoltaics, photovoltaics.

## Abstract

Very thin, thermally evaporated MoO<sub>x</sub> ( $x < 3$ ) layer has been used as transparent hole-selective contact on an n-type Germanium substrate to effectively demonstrate PV conversion capability. The fabricated MoO<sub>x</sub>/Ge heterojunction PV cell shows a photocurrent density of 44.8 mA/cm<sup>2</sup> under AM1.5G illumination, which is comparable to that of conventional Ge PV cells. However, a low open-circuit voltage of 138 mV is obtained, which might be explained by the presence of tunnelling mechanisms through the MoO<sub>x</sub>/Ge interface. To our knowledge, this is the first demonstration of a hole-selective contact made of transition metal oxide on an n-type semiconductor different from c-Si. Thus, this work may have important implications toward the development of new device architectures, such as novel low-cost Ge PV cells with possible applications in multijunction solar cells and thermophotovoltaics.

## Main text

Historically, the driving force for the use of Ge in photovoltaic (PV) applications has been as a substrate for GaAs space solar cells (Miller and Harris 1980), the main reason being the higher thermal conductivity and the possibility of manufacturing thinner and lighter wafers with Ge than with GaAs. Later on, Ge/GaAs tandem solar cells were pursued to enhance the conversion efficiency (Chand et al. 1986) by using the Ge bottom cell to convert the infrared part of the solar spectrum. This progress eventually derived in the development of the current standard technology for space solar cells that consists of triple junction Ge/GaAs/GaInP structures, with AM0 conversion efficiencies in the range of 28-30%. These cells have been also used in terrestrial applications within concentrated-PV (CPV) systems, where they reached AM1.5D conversion efficiencies of 41.6% (R.R. King et al. 2009), just slightly below the current world-

33 record for solar-to-electricity conversion efficiency of 46.0% (Dimroth et al. 2014). Apart from  
34 solar applications, Ge PV cells have been considered as a low-cost replacement for low band  
35 gap III-V semiconductors in thermophotovoltaic (TPV) converters, in which thermal radiation is  
36 directly converted into electricity by infrared sensitive PV devices (Bauer 2011; Chubb 2007).  
37 In this context, Ge TPV cells could be used in a broad range of applications such as waste heat  
38 recovery (Bauer et al. 2003), solar-thermal power (Ungaro, Gray, and Gupta 2015; Lenert et al.  
39 2014; Alejandro Datas and Algora 2013), space power (A. Datas and Martí 2017), and energy  
40 storage (Alejandro Datas et al. 2016), among many others.

41 Current state of the art of Ge PV cells consist of p-n junctions created by diffusion of dopants at  
42 high temperatures (Bitnar 2003). For instance, p-n junctions in p-Ge have been created by  
43 diffusion of V-group atoms (typically P and As) during the first growing step of GaInP or GaAs  
44 nucleation layers within a Metal-Organic CVD (MOCVD) reactor at temperatures of  $\sim 650^{\circ}\text{C}$   
45 (Fernandez et al. 2008; Fernández 2010; Barrigón Montañés 2014). Other groups have used the  
46 diffusion of Zn in n-Ge substrates within a LPE reactor (Khvostikov et al. 2002). In an effort to  
47 reduce manufacturing costs of standalone Ge PV cells, IMEC reported devices with p-n  
48 junctions created by spin-on diffusion of P on p-Ge by rapid thermal annealing at different  
49 temperatures (450-700  $^{\circ}\text{C}$ ) (Posthuma et al. 2007; van der Heide 2009; van der Heide et al.  
50 2009) leading to the best reported 1-sun AM1.5G conversion efficiency for stand-alone Ge PV  
51 cells of 7.9% (van der Heide et al. 2009). Surface passivation has been accomplished by  
52 forming different kinds of heterojunctions on Ge surface, such as Ge/GaAs (Khvostikov et al.  
53 2002) or Ge/GaInP (Fernandez et al. 2008; Fernández 2010; Barrigón Montañés 2014) by  
54 MOCVD or LPE (Khvostikov et al. 2002), or Ge/a-Si (Posthuma et al. 2007; van der Heide  
55 2009; van der Heide et al. 2009; Posthuma et al. 2005), Ge/SiNx (Nagashima, Okumura, and  
56 Yamaguchi 2007) and Ge/a-Si<sub>x</sub>C<sub>1-x</sub> (Fernandez et al. 2008; Fernández 2010) by PECVD.

57 In order to further reduce the fabrication cost of Ge PV cells, it is desirable to eliminate the high  
58 temperature diffusion, and complex MOCVD or PECVD processes. In this regard, a particularly  
59 appealing option consists of substituting the doping step by carrier-selective coatings with  
60 surface passivation properties that could be deposited at low temperatures. For this purpose,  
61 high electron-affinity transition metal oxides (TMOs) such as MoO<sub>3</sub>, WO<sub>3</sub>, and V<sub>2</sub>O<sub>5</sub>, are very  
62 interesting candidates that have already been found effective to produce hole-selective contacts  
63 on both n-type and p-type c-Si (Gerling et al. 2016; Battaglia et al. 2014; Bullock et al. 2014).

64 In this letter we report a Ge PV cell formed by a thin sub-stoichiometric MoO<sub>x</sub> ( $x < 3$ ) layer on  
65 top of an n-type crystalline Ge (c-Ge) substrate, which behaves as a hole selective contact. To  
66 our knowledge, this is the first demonstration of a hole-selective contact made with a TMO on  
67 an n-type semiconductor different than c-Si. Thus, it might open the door to new device

68 architectures, not only for PV applications, but also in photonics and CMOS electronics, where  
69 the integration of TMOs is being investigated (Sanchez et al. 2016), along with the use of  
70 different semiconductors having higher carrier mobilities and extended spectral response than c-  
71 Si, such as Ge (Reboud et al. 2017; Toriumi and Nishimura 2017).

72 The PV cell structure was fabricated on (100) oriented, Czochralski, n-type Ge substrates ( $\rho=$   
73  $0.37 \Omega\cdot\text{cm}$ , 350  $\mu\text{m}$ -thick). The substrate was cleaned by HCl: H<sub>2</sub>O (33%) immediately prior to  
74 rear side passivation by PECVD of (i/n<sup>+</sup>) a-SiC<sub>x</sub>:H (4/15nm, x~0.2) and a-SiC (80nm) stack  
75 deposited at ~ 300°C. Next, the rear contact was created by laser firing of the a-SiC stack to  
76 produce an array of ~ 60  $\mu\text{m}$  diameter local diffusion points, separated by 600  $\mu\text{m}$  pitch. Laser  
77 firing was accomplished by means of a ~1200 mW,  $\lambda= 1064 \text{ nm}$  Nd/YAG laser system at a  
78 frequency of 4 kHz with 6 pulses per spot, following a similar approach than in (López et al.  
79 2018) . The rear contact was finalized by means of an e-beam evaporated Ti/Pd/Ag metal stack  
80 that provides lateral interconnection between fired points. The hole selective contact was  
81 formed at the front side of the device by means of very thin (nominally 20 nm) MoO<sub>x</sub> layer  
82 thermally evaporated from powdered MoO<sub>3</sub> sources at  $\sim 8 \cdot 10^{-6}$  mbar and a deposition rate of ~  
83  $0.2 \text{ \AA/s}$ . A 75 nm-thick ITO layer was subsequently deposited by RF-Sputtering on top of the  
84 MoO<sub>x</sub> layer to increase lateral electrical conductivity and minimize optical reflectivity. A sketch  
85 of the full PV cell structure and the TEM image of the MoO<sub>x</sub>/ITO interface are shown in Figure  
86 1, where a pronounced inter-diffusivity between the layers is clearly observed. The 1x1 cm<sup>2</sup>  
87 active area of the PV cells was defined by conventional lithographic techniques followed by  
88 mesa etching of the MoO<sub>x</sub>/ITO layers. Finally, the front Ag grid electrode (2  $\mu\text{m}$  thick) was  
89 evaporated through a shadow mask for a 4% contacted area

90 The current density-voltage (*J-V*) curve under 1-sun illumination is shown in Figure 2. The  
91 short-circuit current density ( $J_{\text{SC}}= 44.8 \text{ mA/cm}^2$ ) outperforms that of the best performing state of  
92 the art Ge PV cells ( $43.2 \text{ mA/cm}^2$ ) (van der Heide et al. 2009). On the other hand, a much lower  
93 open circuit voltage (138 mV) is measured, compared to those reported in (Fernández 2010; van  
94 der Heide et al. 2009) (up to 265 mV), which ultimately results in a lower FF (40.9 %), partially  
95 due to a non-optimized metal grid that introduces a series resistance of  $0.65 \Omega\text{cm}^2$ . As a result,  
96 an AM1.5G conversion efficiency of 2.53 % is obtained.

97 External quantum efficiency (EQE) of the PV cell is shown in Figure 3 at short-circuit  
98 conditions along with the EQE of Ge PV cells reported in (van der Heide 2009) for a direct  
99 comparison. The improved EQE for wavelengths shorter than 600 nm might be explained by the  
100 reduction of the recombination close to the front surface compared to the one existing in the  
101 highly-doped emitters ( $10^{19}$ - $10^{21} \text{ cm}^{-3}$ ) used in (van der Heide 2009). Such a low recombination  
102 does not necessary indicate a good chemical surface passivation, i.e. strong reduction of

103 interface state density, but it could be related to a strong electric field that unbalances carrier  
 104 densities, i.e. field-effect passivation. In order to measure the electrostatic potential barrier built  
 105 at the junction ( $V_{bi}$ ), capacitance-voltage measurements in reverse bias were performed  
 106 following the same approach than in (Almora et al. 2017) where similar structures on c-Si  
 107 substrates are characterized. This data can be obtained by fitting the  $C^{-2}$  vs.  $V$  curve, known as  
 108 Mott-Schottky plot, using the following equation  $1/C^2 = 2(V_{bi} - V - 2k_B T/q)/q\epsilon_S N_D$ ,  
 109 where symbols have their usual meanings. By applying this model to the experimental data, we  
 110 get an almost perfect linear fit ( $R^2=0.99988$ ) leading to  $V_{bi} = 317 \pm 4$  mV. Additionally, the  
 111 doping density ( $N_D$ ) can be obtained from the slope of the curves leading to a  $N_D$  value of  
 112  $6.9 \pm 0.1 \cdot 10^{15} \text{ cm}^{-3}$ , which fully agrees with the Ge substrate specifications. The calculated  $V_{bi}$   
 113 indicates that the surface is highly inverted, i.e. hole density at the surface is even higher than  
 114 the doping density  $N_D$ , reducing interface recombination due to the scarce availability of  
 115 electrons. This might explain the relatively high EQE values measured under short-circuit  
 116 conditions in the UV-visible range.

117 In order to investigate the origin of the low  $V_{OC}$ , a further understanding of the current  
 118 mechanisms taking place in the  $\text{MoO}_x/\text{Ge}$  heterojunction is needed. With this aim, open-circuit  
 119 voltage ( $V_{OC}$ ) is measured as a function of photogenerated current ( $J_{ph}$ ) by means of a flash  
 120 lamp. For every flash,  $V_{oc}$  values of the cell are recorded in an oscilloscope, while  $J_{ph}$  is  
 121 estimated from the light intensity measured by a reference Ge PV cell (Kerr, Cuevas, and Sinton  
 122 2001). It is well known that applying the superposition principle and taking into account that the  
 123 device is kept under open-circuit conditions,  $J_{ph}$  must be equal to the current that would be  
 124 measured in the cell at dark conditions and the series resistance has no effect on the  
 125 measurement. As a consequence, the analysis of  $J_{ph}-V_{OC}$  curves enables the extraction of useful  
 126 information otherwise hidden by the series resistance effects in conventional dark  $J-V$   
 127 characteristics. This advantage is crucial in our devices given the combination of relatively high  
 128 currents with significant series resistance. Figure 4 shows the  $J_{ph}-V_{oc}$  curves measured at  
 129 temperatures ranging 293-323 K in 5 K steps. The experimental data are fitted to an exponential  
 130 trend given by  $J_{ph} = J_0(T)[\exp(A(T) \cdot V_{OC}) - 1]$  and two examples for the highest and lowest  
 131 temperature measurement are also shown in Figure 4. Notice that in this model no series  
 132 resistance is included and consequently we have only two free parameters: the saturation current  
 133 density,  $J_0(T)$ , and the exponential factor,  $A(T)$ . In Figure 5 we show the Arrhenius plot of these  
 134 parameters where a constant value of  $A \approx 34 \text{ V}^{-1}$  and an activation energy of 0.462 eV for  $J_0(T)$   
 135 suggests that tunnelling mechanism dominates at the  $\text{MoO}_x/\text{Ge}$  interface (Sze and Ng, n.d.).  
 136 This tunnelling current jeopardizes the electron blocking properties of the junction leading to a  
 137 high saturation current density and, thus, low  $V_{oc}$  values. A deeper knowledge of the band

138 structure and interface characteristics of MoO<sub>x</sub>/Ge junction is needed to fully understand how  
139 this tunnel mechanism takes place and to improve the obtained  $V_{oc}$  values.

140 In conclusion, we have reported for the first time a heterojunction MoO<sub>x</sub>/Ge PV cell that  
141 effectively demonstrates the possibility of creating hole selective contacts in n-type c-Ge.  
142 Photovoltaic performance of the device shows excellent  $J_{sc}$  values (44.8 mA/cm<sup>2</sup>) mainly related  
143 to an enhanced spectral response at short wavelengths. On the other hand, low  $V_{oc}$  values (138  
144 mV) might be explained by an excess of tunnel current at the MoO<sub>x</sub>/Ge interface resulting in  
145 high saturation currents. With evident room for improvement, these results could eventually  
146 open a new route for cost-reduction of Ge-based PV devices, including the development of new  
147 kind of low cost thermophotovoltaic converters. Eventually, it could also open the door for the  
148 integration of transition metal oxides in Ge photonics and CMOS electronics.

#### 149 **Acknowledgements**

150 This work was supported by MINECO (Ministerio de Economía y Competitividad de España)  
151 under Thin-IBC [TEC2017-82305-R], CHENOC [ENE2016-78933-C4-1-R], and TORMES  
152 [ENE2015-72843-EXP] projects, and by the EU project AMADEUS, which has received funds  
153 from the Horizon 2020 research and innovation program, FET-OPEN action, under grant  
154 agreement no. 737054. A.Datas acknowledges postdoctoral fellowship support from the Spanish  
155 "Juan de la Cierva-Incorporación" program (IJCI-2015-23747). The sole responsibility for the  
156 content of this publication lies with the authors. It does not necessarily reflect the opinion of the  
157 European Union. Neither the REA nor the European Commission are responsible for any use  
158 that may be made of the information contained therein.

#### 159 **References**

- 160 Almora, Osbel, Luis G. Gerling, Cristóbal Voz, Ramón Alcobilla, Joaquim Puigdollers, and Germà  
161 García-Belmonte. 2017. "Superior Performance of V2O5 as Hole Selective Contact over  
162 Other Transition Metal Oxides in Silicon Heterojunction Solar Cells." *Solar Energy  
163 Materials and Solar Cells* 168 (August): 221–26.  
164 <https://doi.org/10.1016/j.solmat.2017.04.042>.
- 165 Barrigón Montañés, Enrique. 2014. "Development of GaInP/GaInAs/Ge TRIPLE-Junction Solar  
166 Cells for CPV Applications." Phd, E.T.S.I. Telecomunicación (UPM).  
167 <http://oa.upm.es/30449/>.
- 168 Battaglia, Corsin, Xingtian Yin, Maxwell Zheng, Ian D. Sharp, Teresa Chen, Stephen McDonnell,  
169 Angelica Azcatl, et al. 2014. "Hole Selective MoO<sub>x</sub> Contact for Silicon Solar Cells." *Nano  
170 Letters* 14 (2): 967–71. <https://doi.org/10.1021/nl404389u>.
- 171 Bauer, T. 2011. *Thermophotovoltaics: Basic Principles and Critical Aspects of System Design*.  
172 Green Energy and Technology. Springer.
- 173 Bauer, T., I. Forbes, R. Penlington, and N. Pearsall. 2003. "The Potential of Thermophotovoltaic  
174 Heat Recovery for the Glass Industry." In , edited by J. Coutts Timothy, Guazzoni Guido,  
175 and Luther Joachim, 653:101–10. AIP.

176 Bitnar, Bernd. 2003. "Silicon, Germanium and Silicon/Germanium Photocells for  
177 Thermophotovoltaics Applications." *Semiconductor Science and Technology* 18 (5):  
178 S221. <https://doi.org/10.1088/0268-1242/18/5/312>.

179 Bullock, James, Andres Cuevas, Thomas Allen, and Corsin Battaglia. 2014. "Molybdenum Oxide  
180 MoOx: A Versatile Hole Contact for Silicon Solar Cells." *Applied Physics Letters* 105  
181 (23): 232109. <https://doi.org/10.1063/1.4903467>.

182 Chand, N., J. Klem, T. Henderson, and H. Morkoç. 1986. "Diffusion of As and Ge during Growth  
183 of GaAs on Ge Substrate by Molecular-beam Epitaxy: Its Effect on the Device Electrical  
184 Characteristics." *Journal of Applied Physics* 59 (10): 3601–4.  
185 <https://doi.org/10.1063/1.336790>.

186 Chubb, D. L. 2007. *Fundamentals of Thermophotovoltaic Energy Conversion*. Elsevier.

187 Datas, A., and A. Martí. 2017. "Thermophotovoltaic Energy in Space Applications: Review and  
188 Future Potential." *Solar Energy Materials and Solar Cells* 161 (March): 285–96.  
189 <https://doi.org/10.1016/j.solmat.2016.12.007>.

190 Datas, Alejandro, and Carlos Algora. 2013. "Development and Experimental Evaluation of a  
191 Complete Solar Thermophotovoltaic System." *Progress in Photovoltaics: Research and  
192 Applications* 21 (5): 1025–39. <https://doi.org/10.1002/pip.2201>.

193 Datas, Alejandro, Alba Ramos, Antonio Martí, Carlos del Cañizo, and Antonio Luque. 2016.  
194 "Ultra High Temperature Latent Heat Energy Storage and Thermophotovoltaic Energy  
195 Conversion." *Energy* 107 (July): 542–49. <https://doi.org/10.1016/j.energy.2016.04.048>.

196 Dimroth, F., M. Grave, P. Beutel, and C. Fiedeler. 2014. "Wafer Bonded Four-Junction GaInP /  
197 GaAs // GaInAsP / GaInAs Concentrator Solar Cells with 44.7% Efficiency." *Prog.  
198 Photovolt: Res. Appl* 22: 277–82.

199 Fernández, J. 2010. "Optimization of Crystalline Germanium for Thermophotovoltaic and High-  
200 Efficiency Solar Cells." University Konstanz.

201 Fernandez, J., S. Janz, D. Suwito, E. Oliva, and F. Dimroth. 2008. "Advanced Concepts for High-  
202 Efficiency Germanium Photovoltaic Cells." In *2008 33rd IEEE Photovoltaic Specialists  
203 Conference*, 1–4. <https://doi.org/10.1109/PVSC.2008.4922631>.

204 Gerling, Luis G., Somnath Mahato, Anna Morales-Vilches, Gerard Masmitja, Pablo Ortega,  
205 Cristobal Voz, Ramon Alcubilla, and Joaquim Puigdollers. 2016. "Transition Metal  
206 Oxides as Hole-Selective Contacts in Silicon Heterojunctions Solar Cells." *Solar Energy  
207 Materials and Solar Cells*, Selected papers of the EMRS 2015 Spring meeting –  
208 Symposium C on Advanced Inorganic Materials and Structures for Photovoltaics, 145,  
209 Part 2 (February): 109–15. <https://doi.org/10.1016/j.solmat.2015.08.028>.

210 Heide, J. van der. 2009. "Cost-Efficient Thermophotovoltaic Cells Based on Germanium."  
211 Katholieke Universiteit Leuven.

212 Heide, J. van der, N. E. Posthuma, G. Flamand, W. Geens, and J. Poortmans. 2009. "Cost-  
213 Efficient Thermophotovoltaic Cells Based on Germanium Substrates." *Solar Energy  
214 Materials and Solar Cells* 93 (10): 1810–16.  
215 <https://doi.org/10.1016/j.solmat.2009.06.017>.

216 Kerr, Mark J., Andres Cuevas, and Ronald A. Sinton. 2001. "Generalized Analysis of Quasi-  
217 Steady-State and Transient Decay Open Circuit Voltage Measurements." *Journal of  
218 Applied Physics* 91 (1): 399–404. <https://doi.org/10.1063/1.1416134>.

219 Khvostikov, V. P., O. A. Khostikov, E. V. Oliva, V. D. Rumyantsev, M. Z. Shvarts, T. S. Tabarov,  
220 and V. M. Andreev. 2002. "Zinc-Diffused InAsSbP/InAs and Ge TPV Cells." In  
221 *Conference Record of the Twenty-Ninth IEEE Photovoltaic Specialists Conference, 2002.*,  
222 943–46. <https://doi.org/10.1109/PVSC.2002.1190736>.

223 Lenert, Andrej, David M. Bierman, Youngsuk Nam, Walker R. Chan, Ivan Celanovic, Marin  
224 Soljacic, and Evelyn N. Wang. 2014. "A Nanophotonic Solar Thermophotovoltaic  
225 Device." *Nat Nano* 9 (2): 126–30.

226 López, G., C. Jin, I. Martín, and R. Alcubilla. 2018. "Impact of C-Si Surface Passivating Layer  
227 Thickness on n<sup>+</sup>-Si; Laser-Doped Contacts Based on Silicon Carbide Films." *IEEE*

228 *Journal of Photovoltaics* 8 (4): 976–81.  
 229 <https://doi.org/10.1109/JPHOTOV.2018.2836963>.

230 Miller, D. L., and J. S. Harris. 1980. “Molecular Beam Epitaxial GaAs Heteroface Solar Cell  
 231 Grown on Ge.” *Applied Physics Letters* 37 (12): 1104–6.  
 232 <https://doi.org/10.1063/1.91889>.

233 Nagashima, Tomonori, Kenichi Okumura, and Masafumi Yamaguchi. 2007. “A Germanium Back  
 234 Contact Type Thermophotovoltaic Cell.” *AIP Conference Proceedings* 890 (1): 174–81.  
 235 <https://doi.org/10.1063/1.2711734>.

236 Posthuma, N. E., G. Flamand, W. Geens, and J. Poortmans. 2005. “Surface Passivation for  
 237 Germanium Photovoltaic Cells.” *Solar Energy Materials and Solar Cells* 88 (1): 37–45.  
 238 <https://doi.org/10.1016/j.solmat.2004.10.005>.

239 Posthuma, N. E., J. van der Heide, G. Flamand, and J. Poortmans. 2007. “Emitter Formation and  
 240 Contact Realization by Diffusion for Germanium Photovoltaic Devices.” *IEEE*  
 241 *Transactions on Electron Devices* 54 (5): 1210–15.  
 242 <https://doi.org/10.1109/TED.2007.894610>.

243 Reboud, V., A. Gassenq, J. M. Hartmann, J. Widiez, L. Virot, J. Aubin, K. Guillo, et al. 2017.  
 244 “Germanium Based Photonic Components toward a Full Silicon/Germanium Photonic  
 245 Platform.” *Progress in Crystal Growth and Characterization of Materials* 63 (2): 1–24.  
 246 <https://doi.org/10.1016/j.pcrysgrow.2017.04.004>.

247 R.R. King, A. Boca, W. Hong, and X.-Q. Liu, D. Bhusari, D. Larrabee, K.M. Edmondson, D.C. Law,  
 248 C.M. Fetzer, S. Mesropian, N.H. Karam. 2009. “Band-Gap-Engineered Architectures for  
 249 High-Efficiency Multijunction Concentrator Solar Cells.” In .  
 250 <https://doi.org/10.4229/24thEUPVSEC2009-1AO.5.2>.

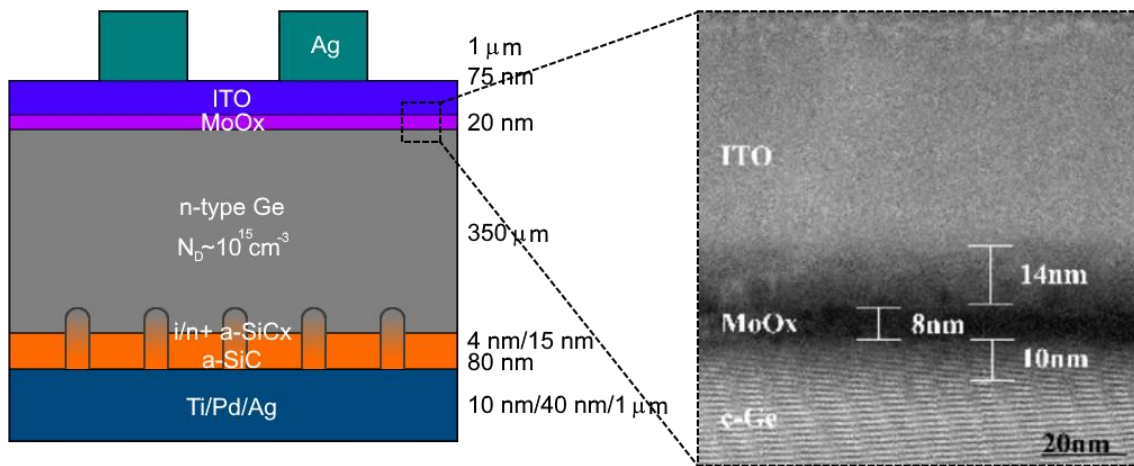
251 Sanchez, L., S. Lechago, A. Gutierrez, and P. Sanchis. 2016. “Analysis and Design Optimization  
 252 of a Hybrid VO<sub>2</sub>/Silicon 2 x 2 Microring Switch.” *IEEE Photonics Journal* 8 (2): 1–9.  
 253 <https://doi.org/10.1109/JPHOT.2016.2551463>.

254 Sze, S.M., and K. K. Ng. n.d. *Physics of Semiconductor Devices*. 3ed ed. John Wiley & Sons.

255 Toriumi, Akira, and Tomonori Nishimura. 2017. “Germanium CMOS Potential from Material  
 256 and Process Perspectives: Be More Positive about Germanium.” *Japanese Journal of*  
 257 *Applied Physics* 57 (1): 010101. <https://doi.org/10.7567/JJAP.57.010101>.

258 Ungaro, Craig, Stephen K. Gray, and Mool C. Gupta. 2015. “Solar Thermophotovoltaic System  
 259 Using Nanostructures.” *Optics Express* 23 (19): A1149.  
 260 <https://doi.org/10.1364/OE.23.0A1149>.

261

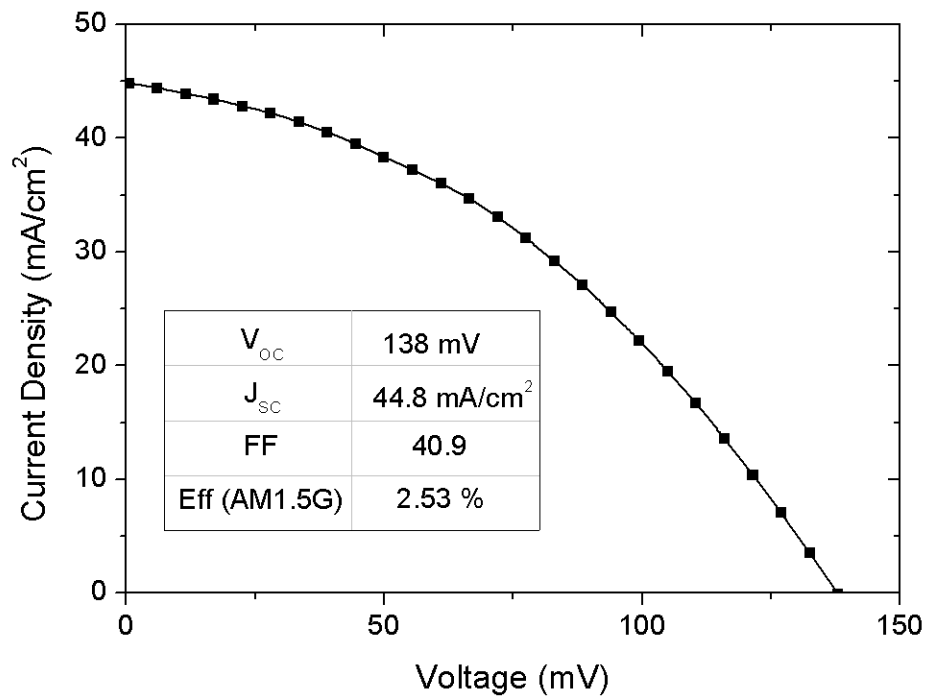


262

263

264 Figure 1. Sketch of the fabricated solar cell. Focus: TEM image of the MoOx interlayer of the  
265 final device

266



267

268 Figure 2. Current density-voltage curve of the Ge PV cell manufactured in this work under  
 269 AM1.5 G illumination conditions.

270

271

272

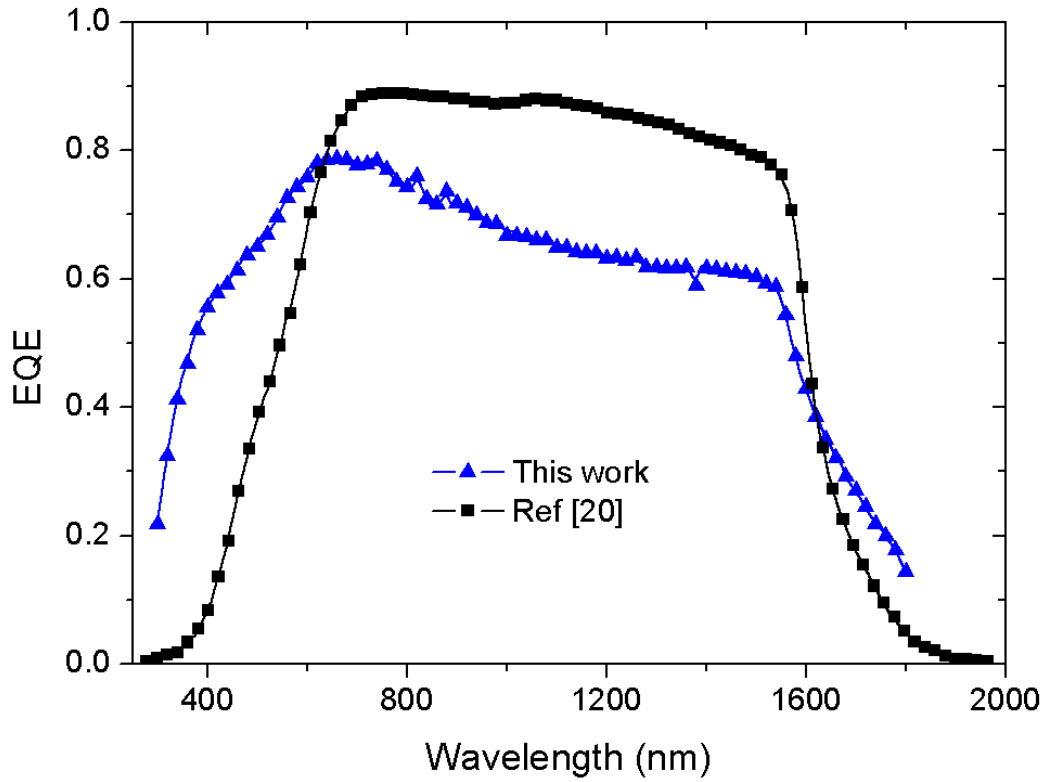
273

274

275

276

277

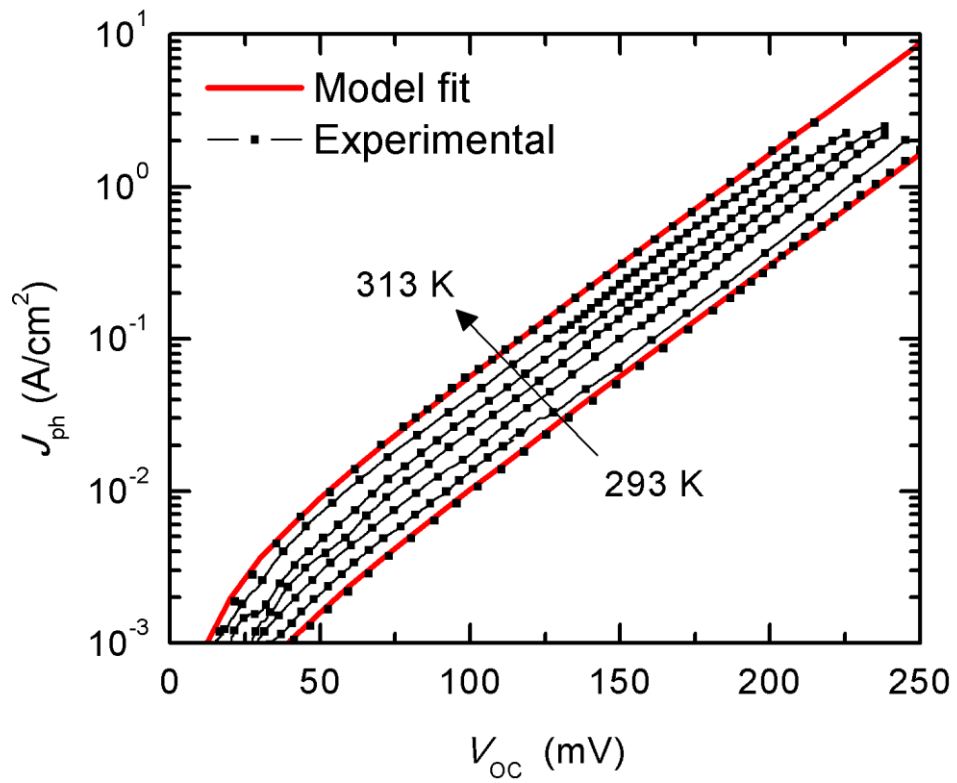


278

279 Figure 3. External quantum efficiency of the Ge PV cell manufactured in this work along with  
 280 that of the Ge PV cell reported in (van der Heide 2009).

281

282

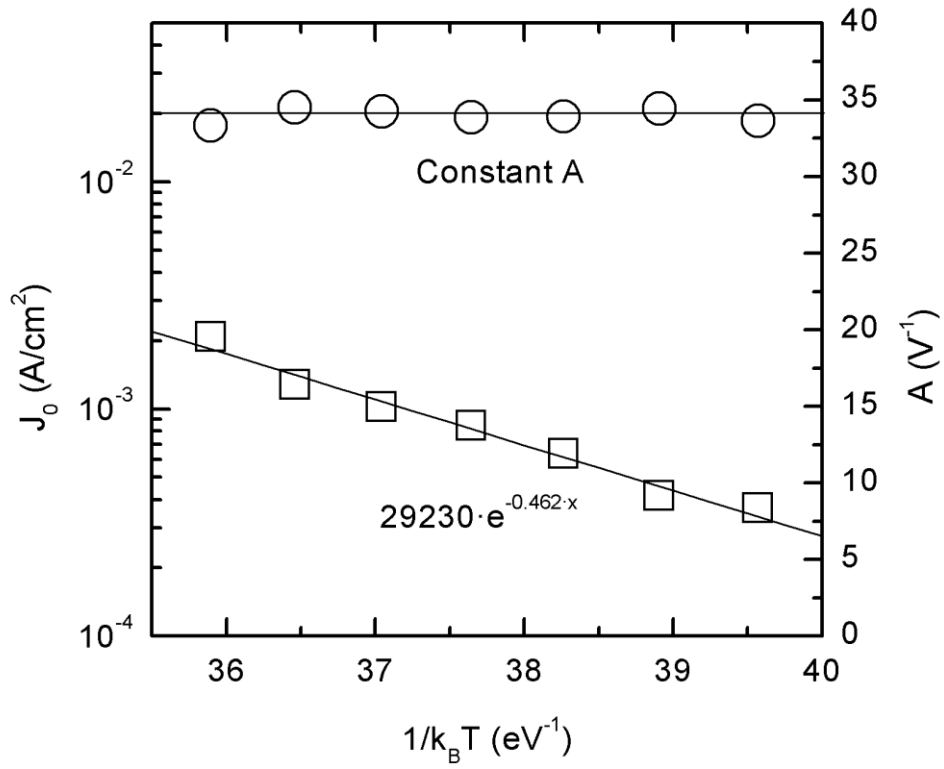


283

284

Figure 4.  $J_{ph}$ - $V_{OC}$  curves at different temperatures from 293 to 333 K in 5 K steps.

285



286

287

Figure 5. Activation energy and current as a function of temperature